Observation of the Semileptonic Decay D-0 -> a(0)(980)(-)e(+)nu(e) and Evidence for D+ -> a(0)(980)(0)e(+)nu(e)

BESIII Collaboration; Haddadi, Zahra; Kalantar-Nayestanaki, Nasser; Kavatsyuk, Myroslav; Messchendorp, Johannes; Tiemens, Marcel

Published in:
Chinese physics c

DOI:
10.1103/PhysRevLett.121.081802

Publication date:
2018

Observation of the Semileptonic Decay $D^0 \to a_0(980)^- e^+ \nu_e$ and Evidence for $D^+ \to a_0(980)^0 e^+ \nu_e$

M. Ablikim,[1] M. N. Achasov,[10,d] S. Ahmed,[15] M. Albrecht,[4] M. Alekseev,[55a,55c] A. Amoroso,[55a,55c] F. F. An,[1] Q. An,[52,42] Y. Bai,[41] O. Bakina,[27] R. Baldini Ferroli,[23a] Y. Ban,[35] K. Begzsuren,[25] D. W. Bennett,[22] J. V. Bennett,[5] N. Berger,[26] M. Bertani,[23a] D. Bettoni,[24a] F. Bianchi,[55a,55c] E. Boger,[27,b] I. Boyko,[27] R. A. Briere,[5] H. Cai,[57] X. Cai,[1,42] A. Calcaterra,[23a] G. F. Cao,[1,46] S. A. Cetin,[45b] J. Chai,[55c] J. F. Chang,[1,42] W. L. Chang,[1,46] G. Chelkov,[27,b,c] G. Chen,[1] H. S. Chen,[1,46] J. C. Chen,[1] M. L. Chen,[1,42] S. J. Chen,[33] X. R. Chen,[30] Y. B. Chen,[1,42] W. Cheng,[55c] X. K. Chu,[35] G. Cibinetto,[24a] F. Cossio,[55c] H. L. Dai,[1,42] J. P. Dai,[37,h] A. Dbeyssi,[15] D. Dedovich,[27] Z. Y. Deng,[1] A. Denig,[26] I. Denysenko,[27] M. Destefanis,[55a,55c] F. De Mori,[55a,55c] Y. Ding,[31] C. Dong,[34] J. Dong,[1,42] L. Y. Dong,[1,46] M. Y. Dong,[1,42,46] Z. L. Dou,[33] S. X. Du,[60] J. Z. Fan,[44] J. Fang,[1,42] S. S. Fang,[1,46] Y. Fang,[1] R. Farinelli,[24a,24b] L. Fava,[55b,55c] F. Feldbauer,[4] G. Felici,[23a] C. Q. Feng,[52,42] M. Fritsch,[4] C. D. Fu,[1] Q. Gao,[1] X. L. Gao,[52,42] Y. Gao,[44] Y. G. Gao,[6] Z. Gao,[52,42] B. Garillon,[26] I. Garzia,[24a] A. Gilman,[49] K. Goetzen,[11] L. Gong,[34] W. X. Gong,[1,42] W. Gradl,[26] M. Greco,[55a,55c] L. M. Gu,[33] M. H. Gu,[1,42] Y. T. Gu,[13] A. Q. Guo,[1] L. B. Guo,[32] R. P. Guo,[1,46] Y. P. Guo,[26] A. Guskov,[27] Z. Haddadi,[29] S. Han,[57] X. Q. Hao,[16] F. A. Harris,[47] K. L. He,[1,46] F. H. Heinsius,[4] T. Held,[4] Y. K. Heng,[1,42,46] Z. L. Hou,[1] H. M. Hu,[1,46] J. F. Hu,[37,h] T. Hu,[1,42,46] Y. Hu,[1] G. S. Huang,[52,42] J. S. Huang,[16] X. T. Huang,[36] X. Z. Huang,[33] Z. L. Huang,[31] T. Hussain,[54] W. Ikegami Andersson,[56] W. Imoehl,[22] M. Irshad,[52,42] Q. Ji,[1] Q. P. Ji,[16] X. B. Ji,[1,46] X. L. Ji,[1,42] H. L. Jiang,[36] X. S. Jiang,[1,42,46] X. Y. Jiang,[34] J. B. Jiao,[36] Z. Jiao,[18] D. P. Jin,[1,42,46] S. Jin,[33] Y. Jin,[48] T. Johansson,[56] N. Kalantar-Nayestanaki,[29] X. S. Kang,[34] M. Kavatsyuk,[29] B. C. Ke,[1] I. K. Keshk,[4] T. Khan,[52,42] A. Khoukaz,[50] P. Kiese,[26] R. Kiuchi,[1] R. Kliemt,[11] L. Koch,[28] O. B. Kolcu,[45b,f] B. Kopf,[4] M. Kuemmel,[4] M. Kuessner,[4] A. Kupsc,[56] M. Kurth,[1] W. Kühn,[28] J. S. Lange,[28] P. Larin,[15] L. Lavezzi,[55c] S. Leiber,[4] H. Leithoff,[26] C. Li,[56] Cheng Li,[52,42] D. M. Li,[60] F. Li,[1,42] F. Y. Li,[35] G. Li,[1] H. B. Li,[1,46] H. J. Li,[1,46] J. C. Li,[1] J. W. Li,[40] K. J. Li,[43] Kang Li,[14] Ke Li,[1] L. K. Li,[1] Lei Li,[3] P. L. Li,[52,42] P. R. Li,[46,7] Q. Y. Li,[36] W. D. Li,[1,46] W. G. Li,[1] X. L. Li,[36] X. N. Li,[1,42] X. Q. Li,[34] Z. B. Li,[43] H. Liang,[52,42] Y. F. Liang,[39] Y. T. Liang,[28] G. R. Liao,[12] L. Z. Liao,[1,46] J. Libby,[21] C. X. Lin,[43] D. X. Lin,[15] B. Liu,[37,h] B. J. Liu,[1] C. X. Liu,[1] D. Liu,[52,42] D. Y. Liu,[37,h] F. H. Liu,[38] Fang Liu,[1] Feng Liu,[6] H. B. Liu,[13] H. L. Liu,[41] H. M. Liu,[1,46] Huanhuan Liu,[1] Huihui Liu,[17] J. B. Liu,[52,42] J. Y. Liu,[1,46] K. Y. Liu,[31] Ke Liu,[6] L. D. Liu,[35] Q. Liu,[46] S. B. Liu,[52,42] X. Liu,[30] Y. B. Liu,[34] Z. A. Liu,[1,42,46] Zhiqing Liu,[26] Y. F. Long,[35] X. C. Lou,[1,42,46] H. J. Lu,[18] J. G. Lu,[1,42] Y. Lu,[1] Y. P. Lu,[1,42] C. L. Luo,[32] M. X. Luo,[59] P. W. Luo,[43] T. Luo,[9,j] X. L. Luo,[1,42] S. Lusso,[55c] X. R. Lyu,[46] F. C. Ma,[31] H. L. Ma,[1] L. L. Ma,[36] M. M. Ma,[1,46] Q. M. Ma,[1] X. N. Ma,[34] X. Y. Ma,[1,42] Y. M. Ma,[36] F. E. Maas,[15] M. Maggiora,[55a,55c] S. Maldaner,[26] Q. A. Malik,[54] A. Mangoni,[23b] Y. J. Mao,[35] Z. P. Mao,[1] S. Marcello,[55a,55c] Z. X. Meng,[48] J. G. Messchendorp,[29] G. Mezzadri,[24a] J. Min,[1,42] T. J. Min,[33] R. E. Mitchell,[22] X. H. Mo,[1,42,46] Y. J. Mo,[6] C. Morales Morales,[15] N. Yu. Muchnoi,[10,d] H. Muramatsu,[49] A. Mustafa,[4] S. Nakhoul,[11,g] Y. Nefedov,[27] F. Nerling,[11,g] I. B. Nikolaev,[10,d] Z. Ning,[1,42] S. Nisar,[8] S. L. Niu,[1,42] X. Y. Niu,[1,46] S. L. Olsen,[46] Q. Ouyang,[1,42,46] S. Pacetti,[23b] Y. Pan,[52,42] M. Papenbrock,[56] P. Patteri,[23a] M. Pelizaeus,[4] J. Pellegrino,[55a,55c] H. P. Peng,[52,42] Z. Y. Peng,[13] K. Peters,[11,g] J. Pettersson,[56] J. L. Ping,[32] R. G. Ping,[1,46] A. Pitka,[4] R. Poling,[49] V. Prasad,[52,42] M. Qi,[33] T. Y. Qi,[2] S. Qian,[1,42] C. F. Qiao,[46] N. Qin,[57] X. S. Qin,[4] Z. H. Qin,[1,42] J. F. Qiu,[1] S. Q. Qu,[34] K. H. Rashid,[54,i] C. F. Redmer,[26] M. Richter,[4] M. Ripka,[26] A. Rivetti,[55c] M. Rolo,[55c] G. Rong,[1,46] Ch. Rosner,[15] M. Rump,[50] A. Sarantsev,[27,e] M. Savrié,[24b] K. Schoenning,[56] W. Shan,[19] X. Y. Shan,[52,42] M. Shao,[52,42] C. P. Shen,[2] P. X. Shen,[34] X. Y. Shen,[1,46] H. Y. Sheng,[1] X. Shi,[1,42] J. J. Song,[36] X. Y. Song,[1] S. Sosio,[55a,55c] C. Sowa,[4] S. Spataro,[55a,55c] F. F. Sui,[36] G. X. Sun,[1] J. F. Sun,[16] L. Sun,[57] S. S. Sun,[1,46] X. H. Sun,[1] Y. J. Sun,[52,42] Y. K. Sun,[52,42] Y. Z. Sun,[1] Z. J. Sun,[1,42] Z. T. Sun,[1] Y. T. Tan,[52,42] C. J. Tang,[39] G. Y. Tang,[1] X. Tang,[1] M. Tiemens,[29] B. Tsednee,[25] I. Uman,[45d] B. Wang,[1] B. L. Wang,[46] C. W. Wang,[33] D. Wang,[35] D. Y. Wang,[35] H. H. Wang,[36] K. Wang,[1,42] L. L. Wang,[1] L. S. Wang,[1] M. Wang,[36] Meng Wang,[1,46] P. Wang,[1] P. L. Wang,[1] W. P. Wang,[52,42] X. F. Wang,[1] Y. Wang,[52,42] Y. F. Wang,[1,42,46] Z. Wang,[1,42] Z. G. Wang,[1,42] Z. Y. Wang,[1] Zongyuan Wang,[1,46] T. Weber,[4] D. H. Wei,[12] P. Weidenkaff,[26] S. P. Wen,[1] U. Wiedner,[4] M. Wolke,[56] L. H. Wu,[1] L. J. Wu,[1,46] Z. Wu,[1,42] L. Xia,[52,42] Y. Xia,[20] Y. J. Xiao,[1,46] Z. J. Xiao,[32] Y. G. Xie,[1,42] Y. H. Xie,[6] X. A. Xiong,[1,46] Q. L. Xiu,[1,42] G. F. Xu,[1] J. J. Xu,[1,46] L. Xu,[1] Q. J. Xu,[14] X. P. Xu,[40] F. Yan,[53] L. Yan,[55a,55c] W. B. Yan,[52,42] W. C. Yan,[2] Y. H. Yan,[20] H. J. Yang,[37,h] H. X. Yang,[1] L. Yang,[57] R. X. Yang,[52,42] S. L. Yang,[1,46] Y. H. Yang,[33] Y. X. Yang,[12] Yifan Yang,[1,46] Z. Q. Yang,[20] M. Ye,[1,42] M. H. Ye,[7] J. H. Yin,[1] Z. Y. You,[43] B. X. Yu,[1,42,46] C. X. Yu,[34] J. S. Yu,[20] C. Z. Yuan,[1,46] Y. Yuan,[1] A. Yuncu,[45b,a] A. A. Zafar,[54] Y. Zeng,[20] B. X. Zhang,[1] B. Y. Zhang,[1,42] C. C. Zhang,[1] D. H. Zhang,[1] H. H. Zhang,[43] H. Y. Zhang,[1,42] J. Zhang,[1,46] J. L. Zhang,[58] J. Q. Zhang,[4] J. W. Zhang,[1,42,46] J. Y. Zhang,[1] J. Z. Zhang,[1,46] K. Zhang,[1,46] L. Zhang,[44] S. F. Zhang,[33] T. J. Zhang,[37,h] X. Y. Zhang,[36]

Y. Zhang,[52,42] Y. H. Zhang,[1,42] Y. T. Zhang,[52,42] Yang Zhang,[1] Yao Zhang,[1] Yu Zhang,[46] Z. H. Zhang,[6] Z. P. Zhang,[52] Z. Y. Zhang,[57] G. Zhao,[1] J. W. Zhao,[1,42] J. Y. Zhao,[1,46] J. Z. Zhao,[1,42] Lei Zhao,[52,42] Ling Zhao,[1] M. G. Zhao,[34] Q. Zhao,[1] S. J. Zhao,[60] T. C. Zhao,[1] Y. B. Zhao,[1,42] Z. G. Zhao,[52,42] A. Zhemchugov,[27,b] B. Zheng,[53] J. P. Zheng,[1,42] Y. H. Zheng,[46] B. Zhong,[32] L. Zhou,[1,42] Q. Zhou,[1,46] X. Zhou,[57] X. K. Zhou,[52,42] X. R. Zhou,[52,42] Xiaoyu Zhou,[20] Xu Zhou,[20] A. N. Zhu,[1,46] J. Zhu,[34] J. Zhu,[43] K. Zhu,[1] K. J. Zhu,[1,42,46] S. H. Zhu,[51] X. L. Zhu,[44] Y. C. Zhu,[52,42] Y. S. Zhu,[1,46] Z. A. Zhu,[1,46] J. Zhuang,[1,42] B. S. Zou,[1] and J. H. Zou[1]

(BESIII Collaboration)

[1]*Institute of High Energy Physics, Beijing 100049, People's Republic of China*
[2]*Beihang University, Beijing 100191, People's Republic of China*
[3]*Beijing Institute of Petrochemical Technology, Beijing 102617, People's Republic of China*
[4]*Bochum Ruhr-University, D-44780 Bochum, Germany*
[5]*Carnegie Mellon University, Pittsburgh, Pennsylvania 15213, USA*
[6]*Central China Normal University, Wuhan 430079, People's Republic of China*
[7]*China Center of Advanced Science and Technology, Beijing 100190, People's Republic of China*
[8]*COMSATS Institute of Information Technology, Lahore, Defence Road, Off Raiwind Road, 54000 Lahore, Pakistan*
[9]*Fudan University, Shanghai 200443, People's Republic of China*
[10]*G.I. Budker Institute of Nuclear Physics SB RAS (BINP), Novosibirsk 630090, Russia*
[11]*GSI Helmholtzcentre for Heavy Ion Research GmbH, D-64291 Darmstadt, Germany*
[12]*Guangxi Normal University, Guilin 541004, People's Republic of China*
[13]*Guangxi University, Nanning 530004, People's Republic of China*
[14]*Hangzhou Normal University, Hangzhou 310036, People's Republic of China*
[15]*Helmholtz Institute Mainz, Johann-Joachim-Becher-Weg 45, D-55099 Mainz, Germany*
[16]*Henan Normal University, Xinxiang 453007, People's Republic of China*
[17]*Henan University of Science and Technology, Luoyang 471003, People's Republic of China*
[18]*Huangshan College, Huangshan 245000, People's Republic of China*
[19]*Hunan Normal University, Changsha 410081, People's Republic of China*
[20]*Hunan University, Changsha 410082, People's Republic of China*
[21]*Indian Institute of Technology Madras, Chennai 600036, India*
[22]*Indiana University, Bloomington, Indiana 47405, USA*
[23a]*INFN Laboratori Nazionali di Frascati, I-00044, Frascati, Italy*
[23b]*INFN and University of Perugia, I-06100, Perugia, Italy*
[24a]*INFN Sezione di Ferrara, I-44122, Ferrara, Italy*
[24b]*University of Ferrara, I-44122, Ferrara, Italy*
[25]*Institute of Physics and Technology, Peace Avenue 54B, Ulaanbaatar 13330, Mongolia*
[26]*Johannes Gutenberg University of Mainz, Johann-Joachim-Becher-Weg 45, D-55099 Mainz, Germany*
[27]*Joint Institute for Nuclear Research, 141980 Dubna, Moscow region, Russia*
[28]*Justus-Liebig-Universitaet Giessen, II. Physikalisches Institut, Heinrich-Buff-Ring 16, D-35392 Giessen, Germany*
[29]*KVI-CART, University of Groningen, NL-9747 AA Groningen, Netherlands*
[30]*Lanzhou University, Lanzhou 730000, People's Republic of China*
[31]*Liaoning University, Shenyang 110036, People's Republic of China*
[32]*Nanjing Normal University, Nanjing 210023, People's Republic of China*
[33]*Nanjing University, Nanjing 210093, People's Republic of China*
[34]*Nankai University, Tianjin 300071, People's Republic of China*
[35]*Peking University, Beijing 100871, People's Republic of China*
[36]*Shandong University, Jinan 250100, People's Republic of China*
[37]*Shanghai Jiao Tong University, Shanghai 200240, People's Republic of China*
[38]*Shanxi University, Taiyuan 030006, People's Republic of China*
[39]*Sichuan University, Chengdu 610064, People's Republic of China*
[40]*Soochow University, Suzhou 215006, People's Republic of China*
[41]*Southeast University, Nanjing 211100, People's Republic of China*
[42]*State Key Laboratory of Particle Detection and Electronics, Beijing 100049, Hefei 230026, People's Republic of China*
[43]*Sun Yat-Sen University, Guangzhou 510275, People's Republic of China*
[44]*Tsinghua University, Beijing 100084, People's Republic of China*
[45a]*Ankara University, 06100 Tandogan, Ankara, Turkey*
[45b]*Istanbul Bilgi University, 34060 Eyup, Istanbul, Turkey*
[45c]*Uludag University, 16059 Bursa, Turkey*
[45d]*Near East University, Nicosia, North Cyprus, Mersin 10, Turkey*

[46]University of Chinese Academy of Sciences, Beijing 100049, People's Republic of China
[47]University of Hawaii, Honolulu, Hawaii 96822, USA
[48]University of Jinan, Jinan 250022, People's Republic of China
[49]University of Minnesota, Minneapolis, Minnesota 55455, USA
[50]University of Muenster, Wilhelm-Klemm-Strasse 9, 48149 Muenster, Germany
[51]University of Science and Technology Liaoning, Anshan 114051, People's Republic of China
[52]University of Science and Technology of China, Hefei 230026, People's Republic of China
[53]University of South China, Hengyang 421001, People's Republic of China
[54]University of the Punjab, Lahore-54590, Pakistan
[55a]University of Turin, I-10125, Turin, Italy
[55b]University of Eastern Piedmont, I-15121, Alessandria, Italy
[55c]INFN, I-10125, Turin, Italy
[56]Uppsala University, Box 516, SE-75120 Uppsala, Sweden
[57]Wuhan University, Wuhan 430072, People's Republic of China
[58]Xinyang Normal University, Xinyang 464000, People's Republic of China
[59]Zhejiang University, Hangzhou 310027, People's Republic of China
[60]Zhengzhou University, Zhengzhou 450001, People's Republic of China

(Received 12 March 2018; revised manuscript received 20 June 2018; published 24 August 2018)

Using an e^+e^- collision data sample of 2.93 fb^{-1} collected at a center-of-mass energy of 3.773 GeV by the BESIII detector at BEPCII, we report the observation of $D^0 \to a_0(980)^- e^+\nu_e$ and evidence for $D^+ \to a_0(980)^0 e^+\nu_e$ with significances of 6.4σ and 2.9σ, respectively. The absolute branching fractions are determined to be $\mathcal{B}(D^0 \to a_0(980)^- e^+\nu_e) \times \mathcal{B}(a_0(980)^- \to \eta\pi^-) = [1.33^{+0.33}_{-0.29}(\mathrm{stat}) \pm 0.09(\mathrm{syst})] \times 10^{-4}$ and $\mathcal{B}(D^+ \to a_0(980)^0 e^+\nu_e) \times \mathcal{B}(a_0(980)^0 \to \eta\pi^0) = [1.66^{+0.81}_{-0.66}(\mathrm{stat}) \pm 0.11(\mathrm{syst})] \times 10^{-4}$. This is the first time the $a_0(980)$ meson has been measured in a D^0 semileptonic decay, which would open one more interesting page in the investigation of the nature of the puzzling $a_0(980)$ states.

DOI: 10.1103/PhysRevLett.121.081802

The study of the nature of the light scalar resonances $a_0(980)$ and $f_0(980)$ has long been one of the central problems of nonperturbative QCD, as they are important for understanding the way that chiral symmetry is realized in the low-energy region and, consequently, for understanding confinement physics [1], i.e., the main consequences of QCD in the hadron world [2,3]. The constituent quark model treats the lightest scalar resonances $a_0(980)/f_0(980)$ as conventional $q\bar{q}$ states [4]. However, the structure of these states seems to be more complicated, and they have also been identified with a compact diquark-antidiquark state or a $K\bar{K}$ bound state [5,6], considering that the simple $q\bar{q}$ picture encounters serious difficulties in understanding the mass problem of the light scalar mesons as well as the $a_0(980)$ production in the radiative decay of $\phi \to \gamma a_0(980)$, which turn out to be readily resolved in the tetraquark scenario [7]. On the other hand, a few tetraquark candidates have been recently observed by various experiments [8–10], but these new states have all heavy-heavy quark contents.

The transition of $D \to a_0(980)$ can be naturally decomposed from the lepton pairs in the $c \to de^+\nu_e$ decay, in which final-state interaction is avoided, and only the spectator light quark is related in the formation of the $a_0(980)$. Therefore, of great interest is to search for the $D^0 \to a_0(980)^- e^+\nu_e$ and $D^+ \to a_0(980)^0 e^+\nu_e$, which will provide the information about the $a_0^-(a_0^+) = d\bar{u}(u\bar{d})$ and $a_0^0 = (u\bar{u} - d\bar{d})/\sqrt{2}$ components in the corresponding $a_0(980)$ wave functions due to its clear production mechanism [11]. Furthermore, the experimental search for $D \to a_0(980)e^+\nu_e$ will be crucial to understand the decay dynamics of D mesons.

In this Letter, we present the first observation of the semileptonic decay $D^0 \to a_0(980)^- e^+\nu_e$ and evidence for $D^+ \to a_0(980)^0 e^+\nu_e$. The data sample used in this analysis was collected at center-of-mass energy $\sqrt{s} = 3.773$ GeV [near the nominal mass of the $\psi(3770)$] by the BESIII detector at the BEPCII collider and corresponds to an integrated luminosity of 2.93 fb^{-1} [12].

The BESIII detector is described in detail elsewhere [13]. The detector has a geometrical acceptance of 93% of 4π. It includes a multilayer drift chamber (MDC) for measuring the momenta and specific ionization energy loss (dE/dx) of charged particles, a time-of-flight (TOF) system which contributes to charged particle identification (PID), a CsI(Tl) electromagnetic calorimeter (EMC) for detecting electromagnetic showers, and a muon chamber system designed for muon identification.

A detailed GEANT4-based [14] Monte Carlo (MC) simulation of the BESIII detector is used to determine the detection efficiencies and evaluate the possible background sources. Events are generated by the generator KKMC [15] using EVTGEN [16], with the effects of the beam energy spread and initial-state radiation (ISR) being taken into account. Final-state radiation is treated via the PHOTOS package [17].

A double-tag analysis technique [18] is employed; this takes advantage of D mesons produced via exclusive $D\bar{D}$ pair production in the decay of the $\psi(3770)$ resonance. We reconstruct $\bar{D}$ mesons using specific hadronic decays, producing a sample of single-tag (ST) events. We then search these ST events for the partner D meson undergoing the decay process of interest; successful searches result in our sample of double-tag (DT) events. This strategy suppresses non-$D\bar{D}$ background effectively and provides a measurement of absolute branching fractions independent of the integrated luminosity and the $D\bar{D}$ production cross section. These absolute branching fractions are calculated as

$$\mathcal{B}_{\rm sig} = \frac{N_{\rm sig}^{\rm obs}}{\sum_\alpha N_{\rm tag}^{{\rm obs},\alpha} \epsilon_{\rm tag,sig}^{\alpha} / \epsilon_{\rm tag}^{\alpha}}, \quad (1)$$

in which α denotes the different ST modes, $N_{\rm tag}^{{\rm obs},\alpha}$ is the ST yield for tag mode α, $N_{\rm sig}^{\rm obs}$ is the sum of the DT yields from all ST modes, and $\epsilon_{\rm tag}^{\alpha}$ and $\epsilon_{\rm tag,sig}^{\alpha}$ refer to the corresponding ST efficiency and the DT efficiency for the ST mode α determined by MC simulations. In this approach, most of the systematic uncertainties arising from the ST reconstruction are canceled.

The ST $\bar{D}$ mesons are reconstructed with the following final states: $\bar{D}^0 \to K^+\pi^-$, $K^+\pi^-\pi^0$, $K^+\pi^-\pi^+\pi^-$, and $D^- \to K^+\pi^-\pi^-$, $K^+\pi^-\pi^-\pi^0$, $K_S^0\pi^-$, $K_S^0\pi^-\pi^0$, $K_S^0\pi^+\pi^-\pi^-$, $K^+K^-\pi^-$. The charged particles $K^\pm$ and $\pi^\pm$, as well as the neutral particles π^0 and K_S^0, are selected with the same criteria as those in Ref. [19]. Throughout this Letter, charge-conjugate modes are implied.

Two key kinematic variables, the energy difference $\Delta E \equiv E_D - E_{\rm beam}$ and beam-constrained mass $M_{\rm BC} \equiv \sqrt{E_{\rm beam}^2/c^4 - |\vec{p}_D|^2/c^2}$ are used to identify the ST $\bar{D}$ candidates. Here, $E_{\rm beam}$ is the beam energy, and E_D and $\vec{p}_D$ are the reconstructed energy and momentum of the $\bar{D}$ candidate in the e^+e^- center-of-mass system. For true $\bar{D}$ candidates, ΔE and $M_{\rm BC}$ will peak at zero and the nominal mass of the D meson, respectively. We accept the $\bar{D}$ candidates with $M_{\rm BC}$ greater than 1.83 GeV$/c^2$ and apply mode-dependent ΔE requirements of approximately 3 standard deviations. When multiple candidates exist, at most one candidate per tag mode per charm (i.e., D or $\bar{D}$) is retained in each event by selecting the candidate with the smallest $|\Delta E|$ [20]. The ST yields are determined by performing a maximum likelihood fit to the $M_{\rm BC}$ distributions of the accepted $\bar{D}$ candidates, as shown in Fig. 1. The signal shape is modeled by the MC simulated shape convolved with a Gaussian function with free parameters. The MC simulation includes the effects of beam energy spread, ISR, the $\psi(3770)$ line shape, and experimental resolution, while the Gaussian convolution allows for small imperfections in the MC simulation. The combinatorial background is modeled by an ARGUS function [21]. The ST yield for each mode is calculated by subtracting the integrated combinatorial background yield from the total number of events contained in the signal regions defined as $1.858 < M_{\rm BC} < 1.874$ GeV$/c^2$ for $\bar{D}^0$ and $1.860 < M_{\rm BC} < 1.880$ GeV$/c^2$ for D^-. The ST yields in the data and the corresponding ST efficiencies are listed in Table I.

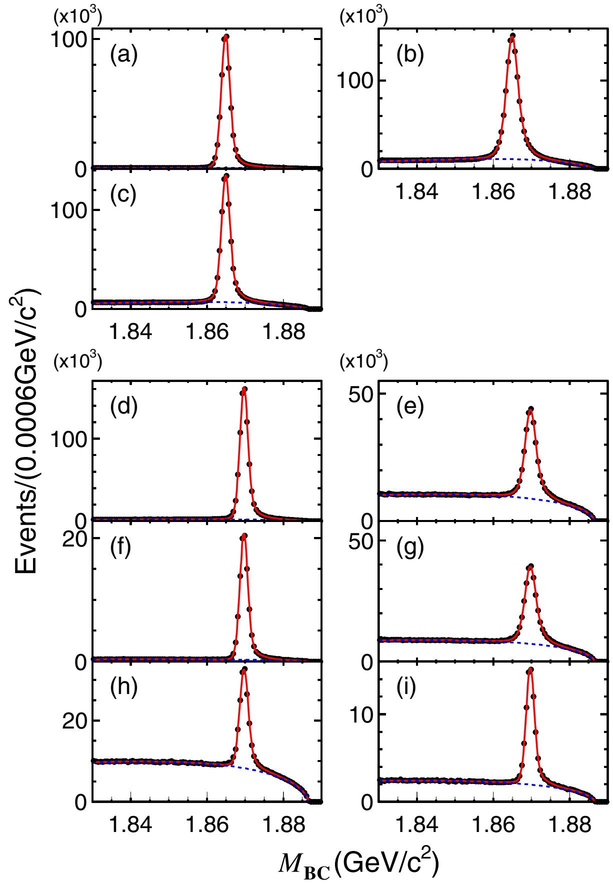

FIG. 1. Fits to the $M_{\rm BC}$ distributions of the ST candidates. The first two rows show the $\bar{D}^0$ modes (a) $K^+\pi^-$, (b) $K^+\pi^-\pi^0$, (c) $K^+\pi^-\pi^+\pi^-$, and the last three rows show the D^- modes (d) $K^+\pi^-\pi^-$, (e) $K^+\pi^-\pi^-\pi^0$, (f) $K_S^0\pi^-$, (g) $K_S^0\pi^-\pi^0$, (h) $K_S^0\pi^+\pi^-\pi^-$, (i) $K^+K^-\pi^-$. Points with error bars represent data, the (red) solid lines are the total fits, and the (blue) dashed lines represent the background contributions.

We search in the selected ST events for the semileptonic decays $D^0 \to a_0(980)^- e^+\nu_e$ and $D^+ \to a_0(980)^0 e^+\nu_e$ using the remaining charged tracks and photon candidates

TABLE I. ST yields in data $N_{\rm tag}^{\rm obs}$, ST efficiencies $\epsilon_{\rm tag}$, and DT efficiencies $\epsilon_{\rm tag,sig}$, with statistical uncertainties, for each mode α. Branching fractions of $K_S^0 \to \pi^+\pi^-$, $\pi^0 \to \gamma\gamma$, and $\eta \to \gamma\gamma$ are not included in the efficiencies. The first three rows are for $\bar{D}^0$ candidates, and the last six rows are for D^- candidates.

Mode	$N_{\rm tag}^{\rm obs,\alpha}$	$\epsilon_{\rm tag}^{\alpha}$ (%)	$\epsilon_{\rm tag,sig}^{\alpha}$ (%)
$K^+\pi^-$	541541 ± 753	65.92 ± 0.02	15.18 ± 0.20
$K^+\pi^-\pi^0$	1040340 ± 1209	34.66 ± 0.01	8.00 ± 0.08
$K^+\pi^-\pi^+\pi^-$	706179 ± 982	38.96 ± 0.01	7.02 ± 0.09
$K^+\pi^-\pi^-$	806444 ± 953	51.08 ± 0.02	5.23 ± 0.07
$K^+\pi^-\pi^-\pi^0$	252088 ± 816	25.91 ± 0.02	2.40 ± 0.06
$K_S^0\pi^-$	100019 ± 337	54.33 ± 0.05	5.55 ± 0.21
$K_S^0\pi^-\pi^0$	235011 ± 759	29.63 ± 0.03	3.10 ± 0.08
$K_S^0\pi^+\pi^-\pi^-$	131815 ± 710	32.49 ± 0.05	2.66 ± 0.10
$K^+K^-\pi^-$	69642 ± 398	40.58 ± 0.06	4.09 ± 0.20

not used for the ST candidate. Here, the $a_0(980)^-$ and $a_0(980)^0$ are reconstructed by their prominent decays to $\eta\pi^-$ and $\eta\pi^0$, respectively. The PID of the charged hadrons (positrons) is accomplished by combining the dE/dx and TOF (dE/dx, TOF, and EMC) information to construct a likelihood $\mathcal{L}_i$ ($\mathcal{L}'_i$) for each of the hypotheses $i = e/\pi/K$. The charged pion candidate is required to satisfy $\mathcal{L}_\pi > \mathcal{L}_K$ and $\mathcal{L}_\pi > 0.1\%$. The positron candidate is required to satisfy $(\mathcal{L}'_e/\mathcal{L}'_e + \mathcal{L}'_\pi + L'_K) > 0.8$ and $E/(pc) > 0.8$, where E is the energy deposited in the EMC, and p is the momentum measured by the MDC. A candidate signal event is required to have a single positron (electron) for signal D ($\bar{D}$) decays. The π^0 and η candidates are formed from pairs of photon candidates with invariant two-photon masses within (0.115, 0.150) and $(0.508, 0.572)$ GeV/c^2, respectively. To improve the kinematic resolution, a one-constraint (1-C) kinematic fit is performed by constraining the $\gamma\gamma$ invariant mass to the expected nominal mass [22]. Background from wrong-pairing photons is suppressed by requiring the decay angle defined as $|\cos\theta_{{\rm decay},\pi^0(\eta)}| = (|E_{\gamma 1} - E_{\gamma 2}|/|\vec{p}_{\pi^0(\eta)}|)$ to be less than 0.80 and 0.95 for the π^0 and η candidates, respectively. Here, $E_{\gamma 1}$ and $E_{\gamma 2}$ are the energies of the two daughter photons of the $\pi^0(\eta)$, and $\vec{p}_{\pi^0(\eta)}$ is the reconstructed momentum of the $\pi^0(\eta)$. The photon energies and $\vec{p}_{\pi^0(\eta)}$ are the results of the kinematic fit. The $a_0(980)^-$ candidate is formed with a charged pion and a selected η candidate. The $a_0(980)^0$ candidate is formed from the combination of π^0 and η candidates with the least $\chi^2_{1{\rm C},\pi^0} + \chi^2_{1{\rm C},\eta}$, where $\chi^2_{1{\rm C},\pi^0}$ and $\chi^2_{1{\rm C},\eta}$ are the χ^2 values of the 1-C kinematic fits of the π^0 and η candidates, respectively. Furthermore, any event with extra unused charged tracks or π^0 candidates are rejected. This π^0 veto suppresses the following backgrounds: $D^0 \to \rho^- e^+\nu_e$ and $D^0 \to K^*(892)^- e^+\nu_e$ [with $K^*(892)^- \to K_S^0\pi^-$] for the $D^0 \to a_0(980)^- e^+\nu_e$ mode; $D^+ \to K_S^0 e^+\nu_e$ and $D^+ \to \bar{K}^*(892)^0 e^+\nu_e$ [with $\bar{K}^*(892)^0 \to K_S^0\pi^0$] for $D^+ \to a_0(980)^0 e^+\nu_e$. In all cases here, $K_S^0 \to \pi^0\pi^0$. Detailed MC studies show that $D^{0(+)} \to K^*(892)^{-(0)} e^+\nu_e$ followed by $\bar{K}^* \to K_L^0\pi$ are prominent backgrounds, where the K_L^0 signal in the EMC can mimic the higher-energy daughter of the η candidate. To suppress these background, the lateral moment [23] of EMC showers, which peaks around 0.15 for real photons but varies from 0 to 0.85 for K_L^0 candidates, is required to be within (0, 0.35) for the higher-energy photon from the η decay. This requirement suppresses about 70% of the K_L^0 backgrounds, while retaining 95% of the signal, and ultimately leads to a limited K_L^0 contribution and a negligible systematic uncertainty.

For the semileptonic signal candidate, the undetected neutrino is inferred by studying the variable $U \equiv E_{\rm miss} - c|\vec{p}_{\rm miss}|$, where $E_{\rm miss}$ and $\vec{p}_{\rm miss}$ are the missing energy and momentum carried by the neutrino from the semileptonic decay. These are calculated as $E_{\rm miss} = E_{\rm beam} - E_{a_0(980)} - E_e$ and $\vec{p}_{\rm miss} = -(\vec{p}_{\rm tag} + \vec{p}_{a_0(980)} + \vec{p}_e)$, respectively, where $E_{a_0(980)}$ (E_e) and $\vec{p}_{a_0(980)}$ ($\vec{p}_e$) are the energy and momentum of $a_0(980)$ (positron), and $\vec{p}_{\rm tag}$ is the momentum of the ST $\bar{D}$ in the center-of-mass frame. We calculate $\vec{p}_{\rm tag} = \hat{p}_{\rm tag}\sqrt{E^2_{\rm beam}/c^2 - M_D^2 c^2}$, where $\hat{p}_{\rm tag}$ is the unit vector in the momentum direction of the ST $\bar{D}$ and M_D is the nominal D mass [22]. The signal candidates are expected to peak around zero in the U distribution and near the $a_0(980)$ mass in the $M_{\eta\pi}$ spectrum.

To obtain the signal yields, we perform two-dimensional (2D) unbinned maximum likelihood fits to the $M_{\eta\pi}$ versus U distributions, combining all tag modes. Projections of the 2D fits are shown in Fig. 2. The signal shape in the U distribution is described by the MC simulation and that in the $M_{\eta\pi}$ distribution is modeled with a usual Flatté formula [24] for the $a_0(980)$ signal. The mass and two coupling constants $g^2_{\eta\pi}$ and $g^2_{K\bar{K}}$ are fixed to 0.990 GeV/c^2, 0.341 (GeV/$c^2)^2$, and 0.304 (GeV/$c^2)^2$ [25], respectively. The backgrounds are divided into three classes: the residual background from semileptonic $D \to \rho, K_S^0$ and K^* decays mentioned previously (bkg I), the partially reconstructed hadronic D decays (bkg II), and the non-$D\bar{D}$ background (bkg III). For each background source in bkg I, the shape and yield are determined by the MC simulation incorporating the corresponding branching fraction [22]. The shape and yield for bkg II are fixed based on the generic $D\bar{D}$ MC sample, in which all particles decay inclusively based on the branching fractions taken from the PDG [22] but with bkg I modes removed. Bkg III from the continuum processes $e^+e^- \to$ light quarks and $\tau^+\tau^-$ is modeled with a MC-determined shape generated with a modified LUND model [26], with the yield determined in the fit. The 2D probability density functions (PDFs) of all these components are constructed by the product of the U and $M_{\eta\pi}$

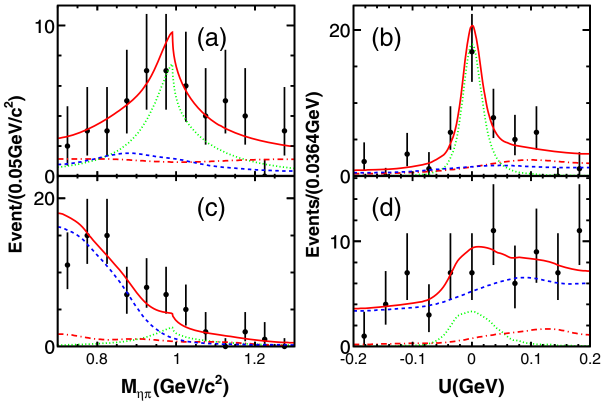

FIG. 2. Projections of the 2D fit on (left) $M_{\eta\pi}$ and (right) U for (a),(b) $D^0 \to a_0(980)^- e^+ \nu_e$ and (c),(d) $D^+ \to a_0(980)^0 e^+ \nu_e$. Points with error bars are data. The (red) solid curves are the overall fits, the (blue) dashed line denotes the sum of the bkg I and bkg II, the (red) dotted-dashed lines denote the bkg III, and the (green) dotted lines show the fitted signal shape.

distributions due to the negligible correlation between the two observables according to the exclusive background channel MC simulation.

The 2D fits yield $25.7^{+6.4}_{-5.7}$ signal events for $D^0 \to a_0(980)^- e^+ \nu_e$ and $10.2^{+5.0}_{-4.1}$ signal events for $D^+ \to a_0(980)^0 e^+ \nu_e$. The statistical significance of the signal taken to be $\sqrt{-2\ln(\mathcal{L}_0/\mathcal{L}_{\rm best})}$, where $\mathcal{L}_{\rm best}$ and $\mathcal{L}_0$ are the maximum likelihood values with the signal yield left free and fixed at zero, respectively, is 6.5σ for $D^0 \to a_0(980)^- e^+ \nu_e$ and 3.0σ for $D^+ \to a_0(980)^0 e^+ \nu_e$. The corresponding DT efficiencies are presented in Table I.

The systematic uncertainties in the measurements are summarized in Table II and discussed below. The uncertainty due to the ST $\bar{D}$ meson largely cancel in the DT analysis method. The uncertainties associated with the tracking and PID for the charged pion are estimated to be 1.0% and 0.5%, respectively, by investigating a control sample $D^+ \to K^- \pi^+ \pi^+$ based on a partial reconstruction technique. Similarly, the uncertainty related with the π^0 reconstruction, including the detection of two photons, is found to be 1.0% by studying the control sample $D^0 \to K^- \pi^+ \pi^0$. Since η candidates are reconstructed similarly, the corresponding uncertainty is also assigned to be 1.0%. The uncertainties related to tracking and PID for the positron are investigated with a radiative Bhabha control sample in the different polar angle and momentum bins. The values for the tracking and PID are 1.0% and 0.6%, respectively, obtained after reweighting according to the distributions of momentum and polar angle of the positron from the signal MC sample. Considering the similar selection criteria of η and π^0, the uncertainty arising from the choice of the best $\eta\pi^0$ combination in the D^+ decay is studied with a di-π^0 sample of DT D hadronic decay, $D^0 \to K^- \pi^+ \pi^0$ versus $\bar{D}^0 \to K^+ \pi^- \pi^0$ and is taken as 0.3% [27].

TABLE II. The relative systematic uncertainties (in %) on the branching fraction measurements. Items marked with $*$ are derived from the fit procedure and are not used when evaluating the upper limit of the branching fraction.

Source	$D^0 \to a_0(980)^- e^+ \nu_e$	$D^+ \to a_0(980)^0 e^+ \nu_e$
Tracking	2.0	1.0
π PID	0.5	⋯
π^0 reconstruction	⋯	1.0
η reconstruction	1.0	1.0
Positron PID	0.6	0.6
The best $\eta\pi^0$ combination	⋯	0.3
Lateral moment requirement	1.6	1.6
Form factor model	5.3	5.6
η and π^0 branching fraction	0.5	0.5
MC statistics	0.6	0.9
$*U$ resolution	2.7	1.1
$*a_0(980)$ line shape	0.2	0.3
*Background modeling	0.3	2.0
Total	6.7	6.6

The efficiency of the lateral moment requirement for photons is studied in different energy and polar angle bins using a control sample of radiative Bhabha events. The average data MC efficiency difference after reweighting according to the energy and polar angle distributions of the signal MC sample is taken as the systematic uncertainty. The form factor of the semileptonic decay for the nominal signal MC sample is parametrized with the model of Ref. [28]. An alternative MC sample based on the Isgur-Scora-Grinstein-Wise (ISGW2) model [29] is produced; the change in the detection efficiency is assigned as the uncertainty associated with the signal model. The uncertainties in the branching fractions of submodes are taken from the current world averages [22]. The effect of limited MC statistics is also included as a systematic effect. Uncertainties associated with the 2D fits are estimated by varying the signal and background shapes and certain background contributions in bkg I and bkg II within their uncertainties. For the resolution of U, the distribution in U of the D^0 decay is convolved with a Gaussian function with free parameters and the fit is redone. Considering the limited statistics and large background contributions, the width of the Gaussian function for the D^+ decay is fixed to be $({\rm FWHM}_+/{\rm FWHM}_0)\sigma_0$, in which σ_0 is the output Gaussian width in the fit to the D^0 case, and ${\rm FWHM}_+$ and ${\rm FWHM}_0$ are the full width at half maximum of the nominal U shape for the D^+ and D^0 signal MC samples, respectively. Changes in the signal yields are assigned to be the corresponding uncertainties. For the $a_0(980)$ line shape, the mass and the two coupling constants in the Flatté formula are varied by 1 standard deviation, and the average change in the signal yield is taken to be the relevant uncertainty. The shapes of the $D\bar{D}$ and non-$D\bar{D}$ backgrounds are modeled using the kernel PDF estimator [30] based on the MC samples with a smoothing parameter set to 1.5. The uncertainties of the shapes are determined by changing the smoothing parameter by ± 0.5, and we take the relative changes on the signal yield as the associated uncertainties. We also shift the yields of bkg I and bkg II in the fits by 1σ calculated from the corresponding branching fractions, luminosity measurements [12], and $D\bar{D}$ cross section [31]. The average changes on the signal yields are taken as the corresponding uncertainties.

Because of the limited statistical significance of the $D^+ \to a_0(980)^0 e^+ \nu_e$ mode, an upper limit on the signal yield is also computed using a Bayesian method. The fit likelihood as a function of the number of signal events denoted as $f_{\mathcal{L}}(N)$ is convolved with Gaussian functions that represent the systematic uncertainties. For all uncertainty sources not from the 2D fit, the effects are modeled by Gaussian functions having widths equal to the corresponding uncertainties. Uncertainties due to the fit procedure are computed using the toy MC simulated events sampled according to the shape of the data. In each toy experiment, we perform a nominal fit and one alternative fit with the shape parameters varied as described above. A Gaussian function is obtained with parameters taken from the mean and the root-mean-square of the resultant discrepancy between the two fitted yields. By integrating up to 90% of the physical region for the smeared $f_{\mathcal{L}}(N)$, we obtain an upper limit of $N^{\rm up} < 18.5$ at the 90% confidence level (C.L.) for the $D^+ \to a_0(980)^0 e^+ \nu_e$ yield.

Since the branching fraction of $a_0(980) \to \eta\pi$ has not been well measured, we report the product branching fractions, obtaining

$$\begin{aligned}&\mathcal{B}(D^0 \to a_0(980)^- e^+ \nu_e) \times \mathcal{B}(a_0(980)^- \to \eta\pi^-)\\ &\quad = (1.33^{+0.33}_{-0.29} \pm 0.09) \times 10^{-4},\\ &\mathcal{B}(D^+ \to a_0(980)^0 e^+ \nu_e) \times \mathcal{B}(a_0(980)^0 \to \eta\pi^0)\\ &\quad = (1.66^{+0.81}_{-0.66} \pm 0.11) \times 10^{-4},\end{aligned}$$

where the first (second) uncertainties are statistical (systematic). The upper limit on the product branching fraction for D^+ decay is determined as $\mathcal{B}(D^+ \to a_0(980)^0 e^+ \nu_e) \times \mathcal{B}(a_0(980)^0 \to \eta\pi^0) < 3.0 \times 10^{-4}$ at the 90% C.L. By convolving the likelihood value from the nominal fits with Gaussian functions whose widths represent the systematic uncertainties for the D^0 and D^+ decays, we calculate the signal significance including systematic uncertainties to be 6.4σ and 2.9σ for the D^0 and D^+ decays, respectively.

To summarize, we present the observation of the semileptonic decay of $D^0 \to a_0(980)^- e^+ \nu_e$ and the evidence for $D^+ \to a_0(980)^0 e^+ \nu_e$. The measured branching fractions are over 2σ deviated from the calculated values based on the QCD light-cone sum rule [32]. Taking the lifetimes of D^0 and D^+ [22] into consideration and assuming that $\mathcal{B}(a_0(980)^- \to \eta\pi^-) = \mathcal{B}(a_0(980)^0 \to \eta\pi^0)$, we find a ratio of partial widths of

$$\frac{\Gamma(D^0 \to a_0(980)^- e^+ \nu_e)}{\Gamma(D^+ \to a_0(980)^0 e^+ \nu_e)} = 2.03 \pm 0.95 \pm 0.06,$$

consistent with the prediction of isospin symmetry, where the shared systematic uncertainties have been canceled. This is the first time the $a_0(980)$ meson has been measured in a D^0 semileptonic decay. Discovery of the $a_0(980)$ in the theoretically clean D^0 semileptonic decay would open one more interesting page in the investigation of the nontrivial nature of the $a_0(980)$ states. Form factor analysis of a future experiment with higher statistics can better uncover the inner structure of $a_0(980)$. Along with the result of the branching fraction of $D^+ \to f_0 e^+ \nu_e$, a result in preparation at BESIII, we will have valuable input for understanding the nature of the light scalar mesons [33].

The BESIII Collaboration thanks the staff of BEPCII and the IHEP computing center for their strong support. This work is supported in part by National Key Basic Research Program of China under Contract No. 2015CB856700; National Natural Science Foundation of China (NSFC) under Contracts No. 11335008, No. 11425524, No. 11625523, No. 11635010, and No. 11735014; the Chinese Academy of Sciences (CAS) Large-Scale Scientific Facility Program; the CAS Center for Excellence in Particle Physics; Joint Large-Scale Scientific Facility Funds of the NSFC and CAS under Contracts No. U1532257, No. U1532258, and No. U1732263; CAS Key Research Program of Frontier Sciences under Contracts No. QYZDJ-SSW-SLH003 and No. QYZDJ-SSW-SLH040; 100 Talents Program of CAS; INPAC and Shanghai Key Laboratory for Particle Physics and Cosmology; German Research Foundation DFG under Contracts No. Collaborative Research Center CRC 1044 and No. FOR 2359; Istituto Nazionale di Fisica Nucleare, Italy; Koninklijke Nederlandse Akademie van Wetenschappen under Contract No. 530-4CDP03; Ministry of Development of Turkey under Contract No. DPT2006K-120470; National Science and Technology Fund; The Swedish Research Council; U.S. Department of Energy under Contracts No. DE-FG02-05ER41374, No. DE-SC-0010118, No. DE-SC-0010504, and No. DE-SC-0012069; University of Groningen and the Helmholtzzentrum fuer Schwerionenforschung GmbH, Darmstadt.

[a]Also at Bogazici University, 34342 Istanbul, Turkey.
[b]Also at the Moscow Institute of Physics and Technology, Moscow 141700, Russia.

[c]Also at the Functional Electronics Laboratory, Tomsk State University, Tomsk, 634050, Russia.
[d]Also at the Novosibirsk State University, Novosibirsk, 630090, Russia.
[e]Also at the NRC "Kurchatov Institute," PNPI, 188300, Gatchina, Russia.
[f]Also at Istanbul Arel University, 34295 Istanbul, Turkey.
[g]Also at Goethe University Frankfurt, 60323 Frankfurt am Main, Germany.
[h]Also at Key Laboratory for Particle Physics, Astrophysics and Cosmology, Ministry of Education and Shanghai Key Laboratory for Particle Physics and Cosmology; Institute of Nuclear and Particle Physics, Shanghai 200240, People's Republic of China.
[i]Also at Government College Women University, Sialkot - 51310, Punjab, Pakistan.
[j]Also at Key Laboratory of Nuclear Physics and Ion-beam Application (MOE) and Institute of Modern Physics, Fudan University, Shanghai 200443, People's Republic of China.

[1] R. L. Jaffe, Phys. Rev. D **15**, 267 (1977).
[2] I. Caprini, G. Colangelo, and H. Leutwyler, Phys. Rev. Lett. **96**, 132001 (2006).
[3] N. N. Achasov and G. N. Shestakov, Phys. Rev. Lett. **99**, 072001 (2007).
[4] D. Morgan and M. R. Pennington, Phys. Rev. D **48**, 1185 (1993).
[5] C. Amsler *et al.* (Particle Data Group), Chin. Phys. C **40**, 100001 (2016).
[6] J. D. Weinstein and N. Isgur, Phys. Rev. D **41**, 2236 (1990).
[7] H. Y. Cheng and C. W. Chiang, Phys. Rev. D **81**, 074031 (2010).
[8] R. Aaij *et al.* (LHCb Collaboration), Phys. Rev. Lett. **112**, 222002 (2014).
[9] M. Ablikim *et al.* (BESIII Collaboration), Phys. Rev. Lett. **115**, 112003 (2015).
[10] M. Ablikim *et al.* (BESIII Collaboration), Phys. Rev. Lett. **115**, 182002 (2015).
[11] N. N. Achasov and A. V. Kiselev, Phys. Rev. D **97**, 036015 (2018); **86**, 114010 (2012); Phys. Part. Nucl. **48**, 681 (2017).
[12] M. Ablikim *et al.* (BESIII Collaboration), Chin. Phys. C **37**, 123001 (2013); Phys. Lett. B **753**, 629 (2016).
[13] M. Ablikim *et al.* (BESIII Collaboration), Nucl. Instrum. Methods Phys. Res., Sect. A **614**, 345 (2010).
[14] S. Agostinelli *et al.* (GEANT4 Collaboration), Nucl. Instrum. Methods Phys. Res., Sect. A **506**, 250 (2003).
[15] S. Jadach, B. F. L. Ward, and Z. Was, Comput. Phys. Commun. **130**, 260 (2000); Phys. Rev. D **63**, 113009 (2001).
[16] D. J. Lange, Nucl. Instrum. Methods Phys. Res., Sect. A **462**, 152 (2001); R. G. Ping, Chin. Phys. C **32**, 599 (2008).
[17] E. Richter-Was, Phys. Lett. B **303**, 163 (1993).
[18] R. M. Baltrusaitis *et al.* (MARK III Collaboration), Phys. Rev. Lett. **56**, 2140 (1986).
[19] M. Ablikim *et al.* (BESIII Collaboration), Phys. Lett. B **744**, 339 (2015).
[20] Q. He *et al.* (CLEO Collaboration), Phys. Rev. Lett. **95**, 121801 (2005).
[21] H. Albrecht *et al.* (ARGUS Collaboration), Phys. Lett. B **241**, 278 (1990).
[22] C. Patrignani *et al.* (Particle Data Group), Chin. Phys. C **40**, 100001 (2016).
[23] A. Drescher, B. Gräwe, B. Hahn, B. Ingelbach, U. Matthiesen, H. Scheck, J. Spengler, and D. Wegener, Nucl. Instrum. Methods Phys. Res., Sect. A **237**, 464 (1985).
[24] S. M. Flatté, Phys. Lett. **63B**, 224 (1976).
[25] M. Ablikim *et al.* (BESIII Collaboration), Phys. Rev. D **95**, 032002 (2017).
[26] J. C. Chen, G. S. Huang, X. R. Qi, D. H. Zhang, and Y. S. Zhu, Phys. Rev. D **62**, 034003 (2000).
[27] M. Ablikim *et al.* (BESIII Collaboration), Chin. Phys. C **40**, 113001 (2016).
[28] D. Becirevic and A. B. Kaidalov, Phys. Lett. B **478**, 417 (2000).
[29] D. Scora and N. Isgur, Phys. Rev. D **52**, 2783 (1995).
[30] K. S. Cranmer, Comput. Phys. Commun. **136**, 198 (2001).
[31] G. Bonvicini *et al.* (CLEO Collaboration), Phys. Rev. D **89**, 072002 (2014).
[32] X. D. Cheng, H. B. Li, B. Wei, Y. G. Xu, and M. Z. Yang, Phys. Rev. D **96**, 033002 (2017).
[33] W. Wang and C. D. Lü, Phys. Rev. D **82**, 034016 (2010).